Adsorption of acrylonitrile on Pt(111) and Au(111) at 95 K in the monolayer and multilayer ranges studied by NEXAFS, UPS, and FT−IR

ARTICLE *in* THE JOURNAL OF PHYSICAL CHEMISTRY · APRIL 1995

Impact Factor: 2.78 · DOI: 10.1021/j100014a028

4 AUTHORS, INCLUDING:

P. Parent
French National Centre for Scientific Research
119 PUBLICATIONS **1,261** CITATIONS

Adsorption of Acrylonitrile on Pt(111) and Au(111) at 95 K in the Monolayer and Multilayer Ranges Studied by NEXAFS, UPS, and FT-IR

Ph. Parent,* C. Laffon, and G. Tourillon

LURE, Centre Universitaire de Paris-Sud, Bât. 209d, 91405 Orsay Cedex, France

A. Cassuto

Laboratoire Maurice Letort, CNRS, Route de Vandœuvre, 54600 Villers lès Nancy, France

Received: July 28, 1994; In Final Form: November 10, 1994[⊗]

We present here UPS, FT-IR, and polarization-dependent NEXAFS measurements at the C(1s) and N(1s) edges of acrylonitrile (CH_2=CH−C≡N) monolayers and multilayers on Pt(111) and Au(111). The NEXAFS results show that the condensed multilayers are almost oriented parallel to the surface. The monolayer formed at 95 K is also oriented flat on the Pt(111) and Au(111) surfaces. The NEXAFS and UPS results show that acrylonitrile is physisorbed on Au(111) and chemisorbed on Pt(111) via the nitrogen lone pair orbital. This orbital hybridizes with the top of the platinum d band, giving rise to an extra antibonding level that is clearly seen on the NEXAFS spectra. The FT-IR results show a low-energy shift of the C≡N stretching vibrational frequency, related to this hybridization.

Introduction

The starting point of this work was to compare the adsorption of acrylonitrile with that of ethylene H_2C=CH_2 and its derivatives on Pt(111)[1−3] to study the effects of the additional nitrile group upon adsorption.

For many unsaturated molecules such as ethylene, the adsorption is very sensitive to the nature and to the orientation of the metal surface. It depends strongly on the hybridizations between the occupied orbitals of the molecule and the vacant bands of the metal, on the hybridizations between the unoccupied orbitals of the molecule and the occupied bands of the metal, and also on the repulsive four-electron interactions between the occupied energy levels of the molecule and the metal.[4] These interactions change with the nature of the metal itself and also with the atomic planes reacting with the molecule. It is then interesting to study the adsorption of acrylonitrile on two surfaces, Au(111) and Pt(111), where the main differences are related to the surface density of states, due to the different filling of the atomic d orbital of Pt ($5d^9$) and Au ($5d^{10}$).

Acrylonitrile simply derives from ethylene by substituting one of the hydrogen atoms with the C≡N group. This additional function modifies the electronic structure of the ethylene group by conjugation between the π orbitals of the C=C and C≡N bonds. This conjugation delocalizes the π(C=C) orbitals over the molecule, lowering the density of electronic states initially located on the C=C group. Therefore we expect a weakening of the reactivity of this bond in the interaction, compared to the case for ethylene. In addition, the nitrile group can directly take part in the adsorption, since this group holds a very active electronic lone pair.

We present here polarization-dependent NEXAFS experiments at the C(1s) and N(1s) edges. This technique gives information on the orientation of the organic layer and on the electronic structure of the unoccupied molecular orbitals. For the two surfaces, the experiments have been done in the multilayer and the monolayer ranges. The study of the multilayer is important to assign the NEXAFS resonances without any influence of the substrate; it is thus a reference for the monolayer spectra. We also present UPS experiments which probe the valence bands of the adsorbed layer. In our case, UPS will give information on the chemical activity of the nitrogen lone pair and on the π orbitals of the molecule, which cannot be seen with NEXAFS spectroscopy which probes only the unfilled states. We have also used XPS (X-ray photoelectron spectroscopy) experiments to determine the carbon and the nitrogen 1s binding energies. They are needed for the interpretation of the NEXAFS transitions: indeed, there are three nonequivalent carbon atoms in acrylonitrile, giving three nonequivalent C(1s) levels from where the photoelectrons could be excited to the same final state. At last, FT-IR experiments on the adsorbates will provide information about the bond strength modifications upon adsorption.

Experimental Section

The NEXAFS experiments have been done at LURE at the Super-ACO storage ring on the SACEMOR beam line (SA72) using a high-energy TGM monochromator (experimental resolution of 90 meV at the carbon edge and 200 meV in the routine mode). UPS (VG, He I radiation, CLAM2 analyzer, pass energy of 2 eV) and XPS (VG, unmonochromatized Mg Kα radiation, pass energy of 10 eV, calibration of the Pt $4f_{7/2}$ level to 71.0 eV) measurements have also been recorded in the SACEMOR experiment using the same sample preparation as for the NEXAFS measurements. Before the depositions, the single crystals (Material Research) cut within 0.5° parallel to the (111) orientation were cleaned using an ion gun sputtering argon at 3.8 kV during 30 min, with simultaneous heating to avoid amorphization (1000 and 700 K for Pt(111) and Au(111), respectively). This procedure was previously checked using both XPS measurements, where no impurities were detected, and low electron energy diffraction (VG) experiments, where sharp (1 × 1) patterns were observed for the gold and the platinum crystals. The crystals were then transferred on the sample holder cooled at 95 K using a liquid nitrogen cryostat. Acrylonitrile (Aldrich) was prepared from grade compound purified by repeated freeze−pump−thaw cycles until the

[⊗] Abstract published in *Advance ACS Abstracts,* March 1, 1995.

0022-3654/95/2099-5058$09.00/0

residual gases were removed. The various dosings were achieved in a special chamber (initial pressure 8×10^{-11} mbar) isolated from the main analysis chamber (pressure 6×10^{-11} mbar) in order to minimize further contamination. Uniform dosings were done using a diffuser outlet located at about 3 cm of the substrate (10^{-8} mbar during 70 s in the isotropic mode for the monolayer and 2×10^{-8} mbar during 20 min for the multilayer in front of the doser). The sample was only transferred in the analysis chamber when the pressure was below 10^{-10} mbar.

The NEXAFS spectra were recorded in about 15 min using two channeltrons collecting the partial secondary electron emission of a clean reference gold grid and that of the sample. The photon energy was calibrated at the carbon K-edge at 284.7 eV using the feature due to the weak contamination of the optics. The NEXAFS spectra presented here in the multilayer range were recorded by collecting the signal of the grid I_g and that of the covered surface I_{cov}; the absorption signal is given by I_{cov}/I_g. In the monolayer range the spectrum of the clean surface (I_{cl}/I_g) was previously recorded before the dosing and then removed from the spectrum of the covered surface (I_{cov}/I_g) by doing the ratio $(I_{cov}/I_g)/(I_{cl}/I_g)$. This method removes artifacts in the spectra due to the contamination of the optics and gives a signal which is only proportional to the adsorbate coverage.[5]

The Fourier transform infrared (FT-IR) spectra of the adsorbates were recorded with a Nicolet 5/20D spectrophotometer, equipped with a liquid nitrogen mercury cadmium telluride (MCT) detector. The IR measurements were taken in the reflection mode (5° between the surface and the IR beam) before and after adsorption of the molecules on the surface. The dosings were made directly in the analysis chamber at 10^{-8} mbar to keep the sample holder at the same position before and after the deposition. The spectra presented here result from the subtraction of the IR spectra of the clean surface from the IR spectra of the covered surface.

Results and Discussion

In the following text, the z axis is chosen perpendicular to the plane (x,y) of the molecule. The three nonequivalent carbon atoms are labeled C_1, C_2, and C_3 (Figure 1). From the XPS measurements recorded on the acrylonitrile multilayer, the binding energies (BE's) have been found at 285.7, 286.6, and 287.4 eV and have been assigned to the C_1, C_2, and C_3 carbon atoms, respectively.[6]

The most intense and narrow features seen on the acrylonitrile NEXAFS spectra correspond to the transitions from the different core levels to the π^* system of the molecule. The π electrons of acrylonitrile are delocalized along the $C_1{=}C_2{-}C_3{\equiv}N$ chain by conjugation between the C=C bond and the C≡N bond.[6] It lifts the degeneracy of the two orthogonal π orbitals of the C≡N group, as observed in the case of propiolic acid.[7] In the z direction, the conjugation gives rise to two bonding π orbitals (namely 1a″ and 2a″ in the C_s point group to which acrylonitrile belongs) and two antibonding π^* orbitals (3a″ and 4a″). We will label the 3a″ level π^*_{1z}(C=C−C≡N) and the 4a″ level π^*_{2z}(C=C−C≡N), or more shortly π^*_{1z} and π^*_{2z}. In the plane (x,y) of the molecule, the π electrons of the C≡N group stay localized on this group (there is no conjugation with the C=C bond for symmetry reasons) and give only one bonding π orbital (12a′) and one antibonding π^* orbital (13a′) labeled π_{xy}(C≡N) and π^*_{xy}(C≡N), respectively. These levels are presented in Figure 1 with the expected NEXAFS transitions from the different initial states (vertical arrows). In this figure, the bold numbers refer to the numbering of the NEXAFS transitions in the spectra presented later (non-underlined, C K-edge; underlined, N K-edge). The dotted arrows are the three allowed transitions $C_1(1s) \rightarrow \pi^*_{xy}$(C≡N), $C_2(1s) \rightarrow \pi^*_{xy}$(C≡N), and $C_1(1s) \rightarrow \pi^*_{2z}$(C=C−C≡N), which are not observed on the NEXAFS spectra due to the weak projection of the final state on the initial state.[6]

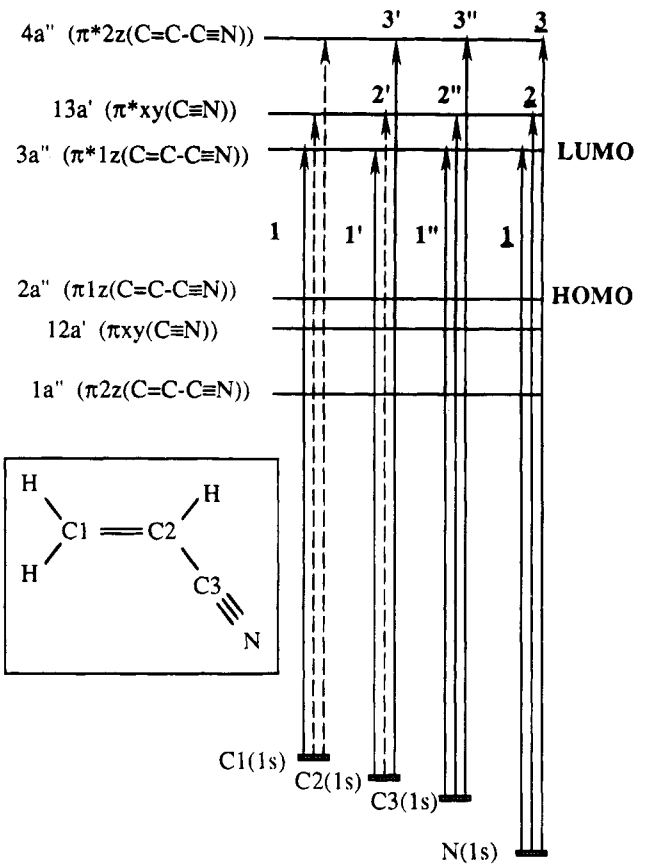

Figure 1. Schematic drawing of the π,π^* system of acrylonitrile with the related NEXAFS transitions (vertical arrows) from the $C_1(1s)$, $C_2(1s)$, $C_3(1s)$, and N(1s) initial states (the inset shows the acrylonitrile molecule). The dotted arrows correspond to the transitions that are not observed on the NEXAFS spectra, due to the weak projection of the final state on the initial state.[6] The underlined and non-underlined bold numbers refer to the labeling of the transitions at the carbon edge and at the nitrogen edge, respectively, used in the text and in the following figures.

The energy domain of the π^* resonances has been fitted using Gaussian functions.[5] We have also reported in the spectra the continuum steps (arctan functions, 1 eV width) located at the ionization potential (IP) values, i.e. the XPS binding energies referenced to the vacuum level. The intensity of each step is simply 1 (the normalization value) divided by the number of carbon atoms at the carbon edge (then 1 at the nitrogen edge).

1. NEXAFS Results for the Acrylonitrile Multilayer. Figures 2 and 3 show the NEXAFS spectra of the acrylonitrile multilayer (50 monolayers) at the carbon edge and at the nitrogen edge, respectively. For the two edges, these spectra have been recorded for two angles between the electric field of the beam and the surface normal (normal incidence, 90°; near grazing incidence, 25°). No differences have been found for the multilayers dosed on Au(111) or Pt(111).

We observe for the two angles a strong polarization dependence of the NEXAFS transitions, showing that the multilayer is oriented on the surface. As shown in Figure 1, the first transition observed at the carbon edge (no. 1 at 284.5 eV) corresponds to the transition from the $C_1(1s)$ level to the LUMO of acrylonitrile, i.e. the π^*_{1z}(C=C−C≡N) (3a″) orbital. The intensity of this transition is greater at grazing incidence than

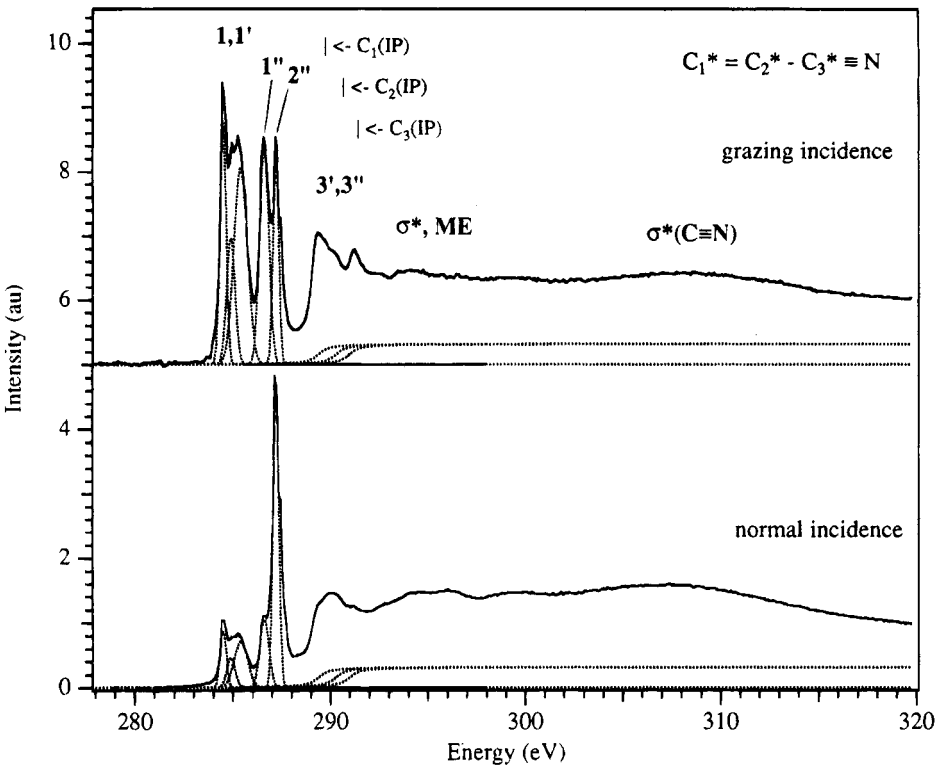

Figure 2. NEXAFS spectra of the acrylonitrile multilayer/Pt(111) or Au(111) at the carbon K-edge.

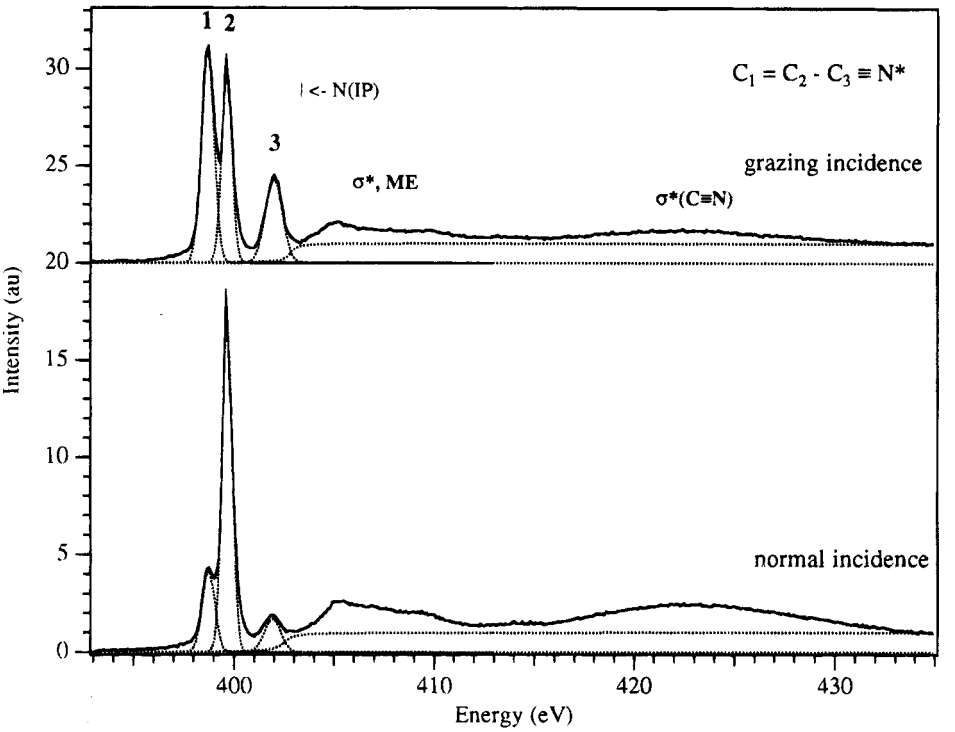

Figure 3. NEXAFS spectra of the acrylonitrile multilayer/Pt(111) or Au(111) at the nitrogen K-edge.

at normal incidence. At the nitrogen edge, the first transition (no. 1 at 398.7 eV) corresponds to excitation from the N(1s) level to the same π^*_{1z} final state; its intensity is also maximized at grazing incidence and minimized at normal incidence. Since the final state π^*_{1z} is perpendicular to the plane of the molecule, it is clear that the molecules are oriented almost flat on the surface.

We describe now in more detail the transitions below the ionization potentials (IP's) for both edges. (i) At the carbon edge (Figure 2), the first peak is strongly broadened by many transitions related to the vibrational envelope of the 3a″ level (a detailed calculation of these fine structures is given in ref 8). The $0 \rightarrow 0$ band of the $C_1(1s) \rightarrow \pi^*_{1z}$ excitation is the narrow feature that appears at 284.5 eV on the left of the peak. As the $C_1(1s)$ and $C_2(1s)$ levels are only separated by 0.9 eV, this peak includes in fact the $C_1(1s) \rightarrow \pi^*_{1z}$ (no. 1) and the $C_2(1s) \rightarrow \pi^*_{1z}$ (no. 1′) transitions. They cannot be resolved, since a lot of vibrational progressions arise from each excitation, so the right tail of the $C_1(1s) \rightarrow \pi^*_{1z}$ transition extends over the $C_2(1s) \rightarrow \pi^*_{1z}$ transition. The three Gaussian functions used for

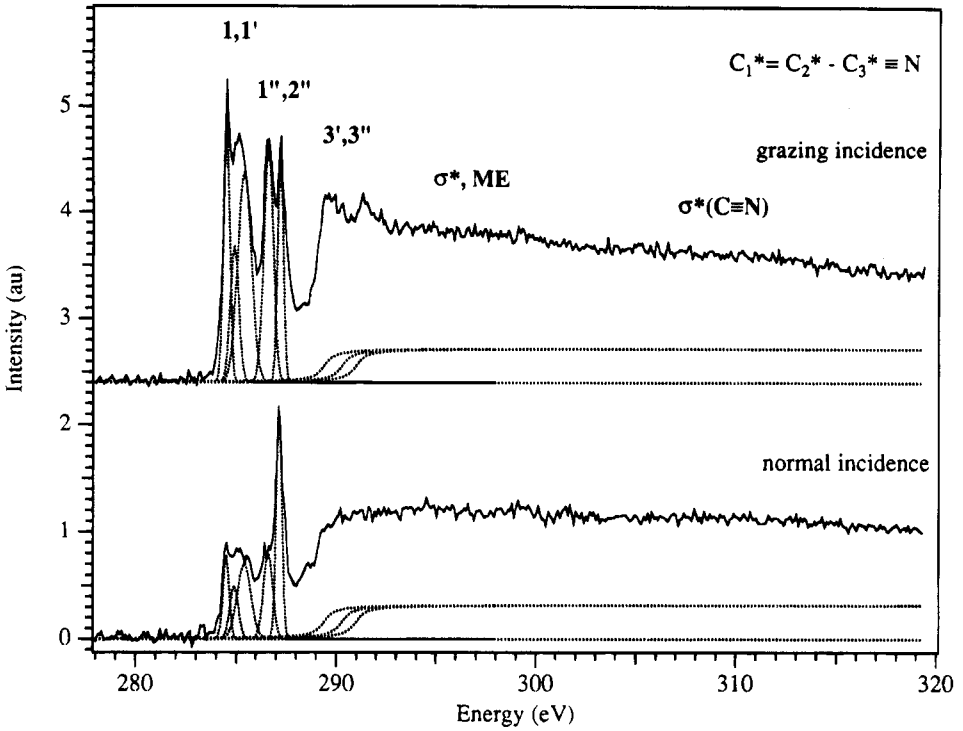

Figure 4. NEXAFS spectra of the acrylonitrile monolayer/Au(111) at the carbon K-edge.

the fitting of this peak have indeed no physical meaning. Just above the first transition, we find the $C_3(1s) \rightarrow \pi^*_{1z}$ excitation (no. 1″ at 286.5 eV), which is separated by 2 eV from the beginning of the no. 1 transition (284.5 eV), as expected from the XPS measurements ($BE(C_3(1s)) - BE(C_1(1s)) = 1.9$ eV). The following transition (no. 2″ at 287.2 eV) corresponds to the $C_3(1s) \rightarrow \pi^*_{xy}$(C≡N) (13a′) excitation. This time, its polarization dependence is reversed compared to that of the $C_{1,2,3} \rightarrow \pi^*_{1z}$ excitations due to the A′ character of the final state. The energy domain around the C_1, C_2, and C_3 IP's is made of numerous transitions that include the transitions $C_2(1s) \rightarrow \pi^*_{2z}$-(C=C—C≡N) (4a″) (no. 3′) and $C_3(1s) \rightarrow \pi^*_{2z}$ (no. 3″). (ii) At the N K-edge (Figure 3), the energy domain below the nitrogen IP is simpler to interpret, since only one core level is involved. The no. 1 transition at 398.7 eV corresponds to the $N(1s) \rightarrow \pi^*_{1z}$(C=C—C≡N) (3a″) excitation, the no. 2 transition at 399.6 eV to the $N(1s) \rightarrow \pi^*_{xy}$(C≡N) (13a′) excitation, and the no. 3 transition at 402.0 eV to the $N(1s) \rightarrow \pi^*_{2z}$-(C=C—C≡N) (4a″) excitation.

Concerning the energy domain above the IP's at both edges, we observe a broad and intense shape resonance with a σ polarization dependence located at 423 eV at the N K-edge and 313 eV at the C K-edge. This resonance lies at the characteristic energies of a σ^* triple-bond orbital in hydrocarbon molecules, so we name it σ^*(C≡N). However, the usual labeling of the "building block" picture[9] (σ^*(C—C), σ^*(C=C), σ^*(C≡N), etc.) loses its meaning for large molecules, since it implies in a sense a localized view of the orbital: for such molecules, the σ^* orbitals extend over all the molecule and cannot be rigorously associated with any functional group. As an example, the first σ^* level ($8a_1$) of acetonitrile (H_3C—C≡N) gives at the carbon edge a shape resonance at the characteristic energy of a σ^*-(C—C) bond, but this orbital strongly overlaps the C≡N bond,[10] so it can be excited also at the nitrogen edge.[11] This is also what is observed at the nitrogen edge of acrylonitrile where at least three resonances are found just above the IP (405, 407, and 409 eV) that include the excitations to the lowest σ^* levels. This energy domain probably also contains multielectronic (ME) excitations ($\pi \rightarrow \pi^*$ shake-up), as observed for acetonitrile.[11] At the carbon edge, we find again many resonances that extend from 293 to 300 eV with complicated shapes that come from the surimposition of the excitations of each core level to the different σ^* levels, probably together with several multielectronic transitions that can occur from the valence band. It is then very difficult to fit the data in order to propose an exact assignment.

2. NEXAFS Results in the Monolayer Range. *a. Acrylonitrile Monolayer on Au(111).* Figures 4 and 5 present the NEXAFS results obtained for one monolayer adsorbed on the Au(111) surface, at the carbon K-edge and at the nitrogen K-edge, respectively. The NEXAFS spectra have been recorded at normal and grazing incidences.

(i) At the carbon K-edge (Figure 4), the C_1, C_2, $C_3 \rightarrow \pi^*_{1z}$ transitions at 284.5 eV (nos. 1 and 1′) and 286.5 eV, as with the $C_3 \rightarrow \pi_{xy}$*(C≡N) one at 287.2 eV (no. 2″), are not modified by the adsorption: their relative intensity and their polarization dependence are roughly similar to those of the multilayer. We still see the vibrational structure of the π^*_{1z} level. We can also observe around the IP the resonances already seen in the multilayer spectra that include transition nos. 3′ and 3″ (C_2, $C_3 \rightarrow \pi^*_{2z}$).

(ii) At the nitrogen K-edge (Figure 5), we observe the N(1s) $\rightarrow \pi^*_{1z}$ transition at 398.7 eV (no. 1), the $N(1s) \rightarrow \pi^*_{xy}$(C≡N) transition at 399.6 eV (no. 2), and the $N(1s) \rightarrow \pi^*_{2z}$ transition at 402.0 eV (no. 3). The polarization dependence of these transitions shows that the molecules are adsorbed, again, nearly parallel to the surface. The width of these resonances is the same as that for the multilayer (0.74, 0.6, and 0.96 eV, respectively). The σ^*(C≡N) shape resonance can be distinguished on the normal incidence spectra with a maximum around 423 eV. As for the multilayer, we observe the small resonances above the IP with roughly the same intensities and the same polarization dependence.

These results show that the monolayer is oriented flat on the surface and that there are no evident modifications of the

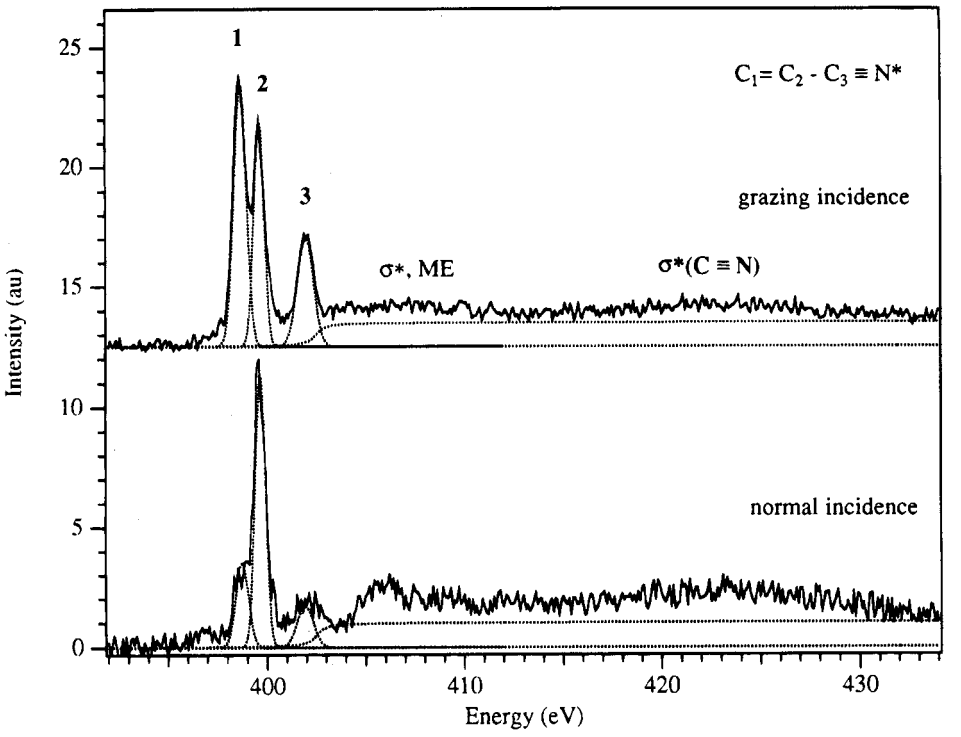

Figure 5. NEXAFS spectra of the acrylonitrile monolayer/Au(111) at the nitrogen K-edge.

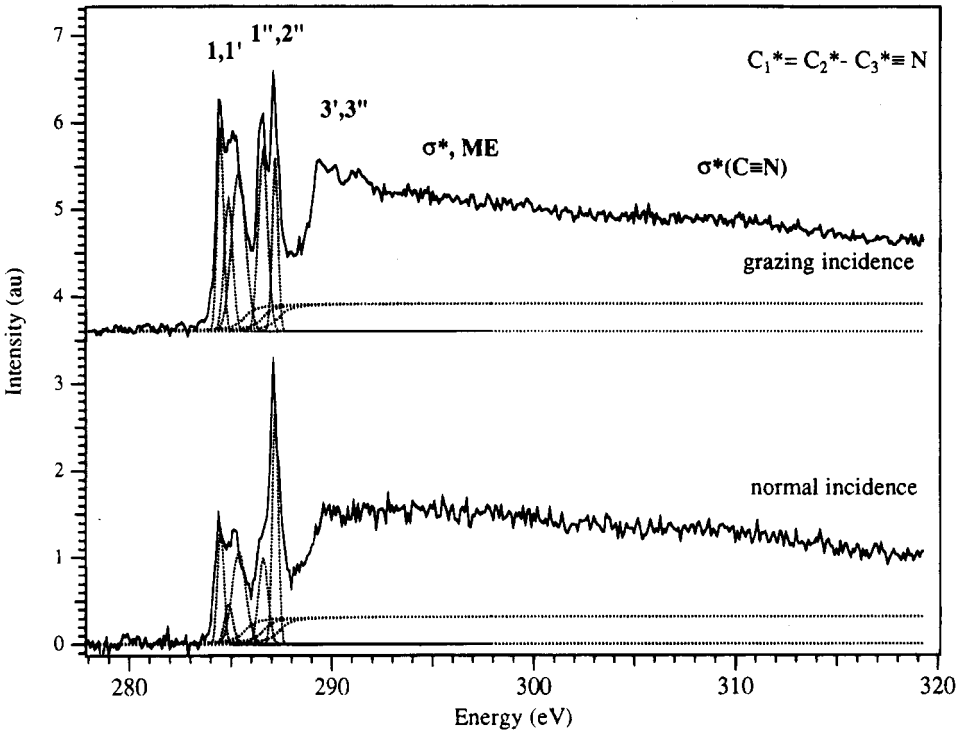

Figure 6. NEXAFS spectra of the acrylonitrile monolayer/Pt(111) at the carbon K-edge.

electronic structure of the molecules compared to the multilayer. Then, acrylonitrile is only physisorbed on Au(111) at 95 K.

b. Acrylonitrile Monolayer on Pt(111). Figures 6 and 7 present the NEXAFS results for the two orientations of a monolayer adsorbed on the Pt(111) surface, at the carbon K-edge and the nitrogen K-edge, respectively.

At the carbon edge (Figure 6) we observe the $C_1, C_2 \rightarrow \pi^*_{1z}$ transitions at 284.5 eV (nos. 1 and 1') still broadened by the vibrational fine structure of the final state. The $C_3 \rightarrow \pi^*_{1z}$ (no. 1" at 286.5 eV) and $C_3 \rightarrow \pi_{xy}^*(C{\equiv}N)$ (no. 2" at 287.2 eV) transitions are also observed, but their intensity ratio with the maximum of the no. 1 transition is slightly different than that for the multilayer or the monolayer/Au(111). This is more evident on the data recorded at grazing incidence. The no. 1" transition involves the same final state as the 1' and 1" ones, so this cannot be due to a change of the orientation compared to the multilayer. The variation of the intensity of the no. 2" transition with respect to the no. 1 transition is also clearly seen at the nitrogen edge (Figure 7).

In the case of chemisorbed species, it is known that the step functions initially located at the vacuum level are shifted to lower energies at positions which coincide with the XPS binding

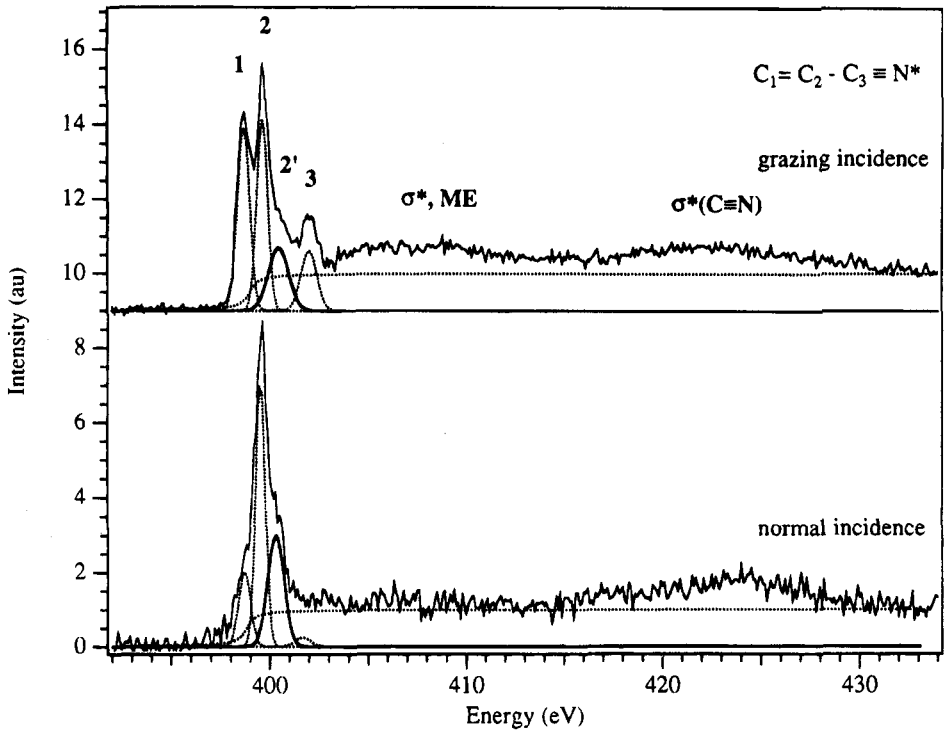

Figure 7. NEXAFS spectra of the acrylonitrile monolayer/Pt(111) at the nitrogen K-edge.

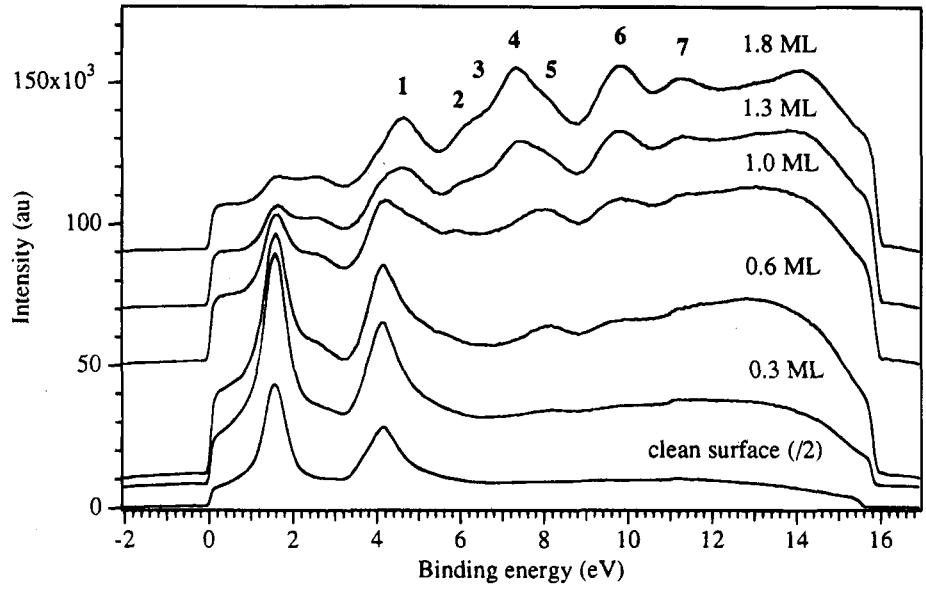

Figure 8. UP (He I) spectra of the acrylonitrile/Pt(111) for increasing coverages.

energies (relative to the Fermi level).[5] Therefore, we have fitted for both edges the π^* resonances with the continuum steps located at the carbon and nitrogen BE's as determined by XPS. This procedure leads to better fits and gives also roughly the same intensity ratio of the no. 1″ or 2″ transitions (and nos. 2 and 3 at the nitrogen edge)—compared to the first transition—as for the multilayer or the monolayer/Au(111). The energy shift of the continuum steps is then the first evidence of a chemisorption process for acrylonitrile/Pt(111). However, the most important evidence for a chemisorption is the intense shoulder that appears to the right of the π_{xy}^*(C≡N) transition—only at the nitrogen edge—with a marked *xy*-polarization dependence (peak no. 2′ at 400.5 eV). The presence of this peak is reliable, since no structure appears in the blank spectrum for the two orientations. It has also been observed for each repeated experiment we have done on Pt(111). Such extrapeaks (or strong π^* broadenings) are quite frequently observed for chemisorbed species and result from the hybridization between a molecular orbital and a localized band of the surface, giving rise to a new antibonding level.

3. UPS Results. Figure 8 gives the UPS spectra (He I) obtained on acrylonitrile adsorbed at 95 K on Pt(111) for different coverages, from the clean surface to 1.8 monolayers (ML). Figure 9 presents the same experiment on Au(111). For the highest coverage, the spectrum contains all the features present in the gas phase,[12-14] but broadened and shifted in energy, due to solid state effects. The first valence levels nos. 1, 2, 3, and 4 are assigned to the π_{1z} (2a″), π_{xy}(C≡N) (12a′), lpN°° (11a′) (the nitrogen lone pair), and π_{2z} (1a″) orbitals, respectively. The deeper bands nos. 5, 6, and 7 have been assigned to the π(CH$_2$) (10a′), σ(C=C) (9a′), and C$_3$(2s) (8a′) orbitals in refs 12 and 14. We have calculated the energy

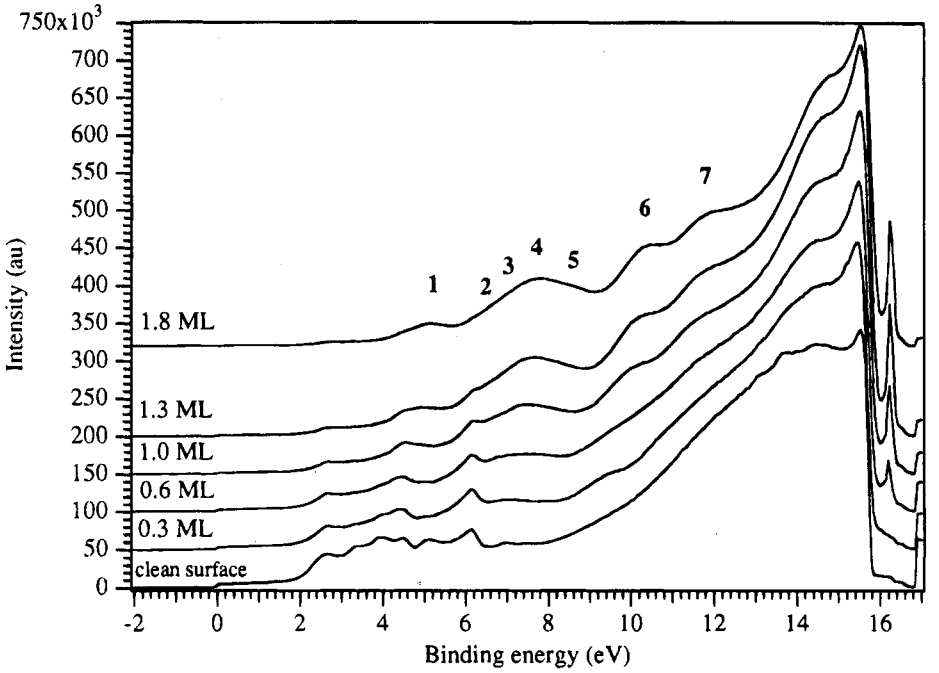

Figure 9. UP (He I) spectra of the acrylonitrile/Au(111) for increasing coverages.

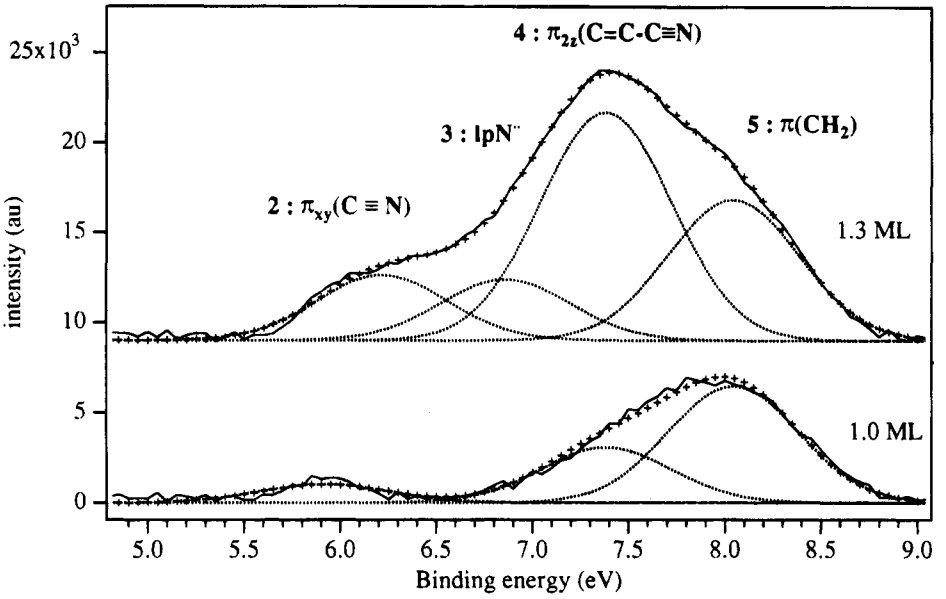

Figure 10. Detail of the UP spectra on Pt(111) (5−9 eV) for the 1 ML and the 1.3 ML coverages.

differences between each successive level for the condensed species, which are roughly the same as for the gas (experimental values taken from ref 12). It confirms that these solid state effects perturb in the same way the energy position of the valence levels, and so the assignment of the transitions holds for the condensed layers.

Figure 10 details the range 5.5−9 eV of the Pt(111) experiments for two coverages (1 ML—that corresponds to the NEXAFS experiments—and 1.3 ML—that corresponds to the appearance of the second layer). For 1.3 ML, we observe clearly the π_{xy}(C≡N), lpN°°, π_{1z}, and π(CH_2) bands, whereas at 1 ML the lpN°° level is not present. Figure 11 details the range 6−9 eV of the Au(111) experiments (for the energy range below 6 eV, the levels are superimposed with the metal bands) for the same coverages (1 ML and 1.3 ML). For 1.3 ML, we observe the lpN°°, π_{1z}, and π(CH_2) bands; contrary to the Pt(111) measurements, these bands are also observed at 1 ML (and for lower coverages).

These results clearly show that, for the monolayer on Pt-(111), the lpN°° level is strongly perturbed by the interaction with the metal. For the monolayer/Au(111), there is no evidence of a modification of the valence levels.

4. FT-IR Results. Figure 12 presents the FT-IR spectra obtained on the Pt(111) surface for 1 ML, 2 ML, and a multilayer (12 ML) in the C≡N stretching domain. Peak B at 2232 cm^{-1} is assigned to the free C≡N group symmetric stretching.[15] At 1 ML, this peak is strongly shifted to lower frequencies (peak A at 2200 cm^{-1}); peak B appears only at 2 ML, where there is still a contribution of the monolayer. For the multilayer, one distinguishes a weak residual peak A and an intense peak B, due to the increasing coverage. Again, these results clearly confirm that acrylonitrile strongly interacts with the Pt(111) surface and that the C≡N group is modified by this interaction. The low-energy shift of the C≡N stretching band indicates a weakening of the C≡N binding energy. Indeed, since the lpN°° orbital slightly extends over the C≡N group,

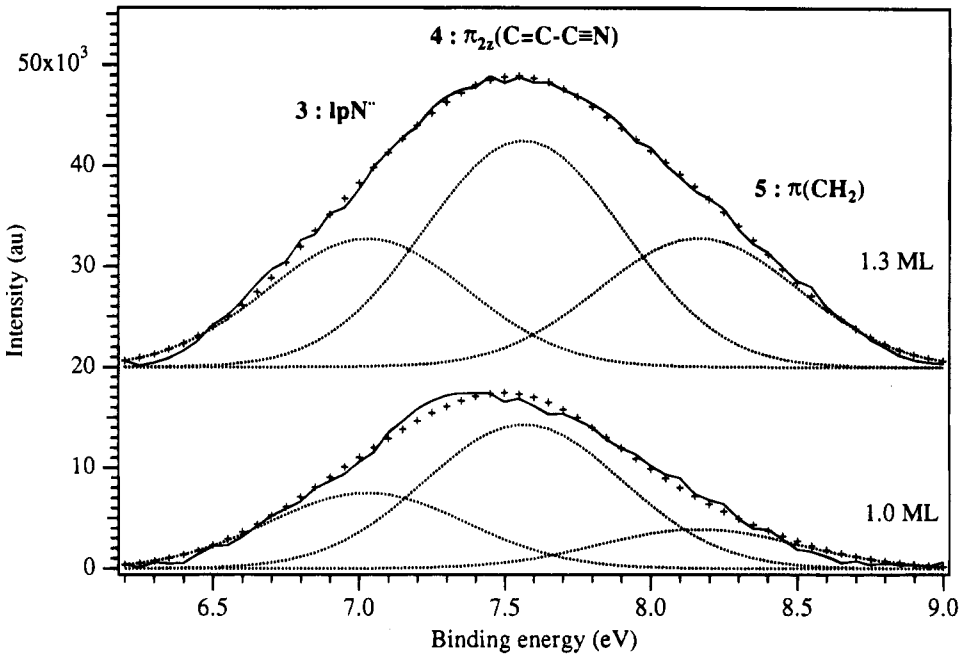

Figure 11. Detail of the UP spectra on Au(111) (6.2−9 eV) for the 1 ML and the 1.3 ML coverages.

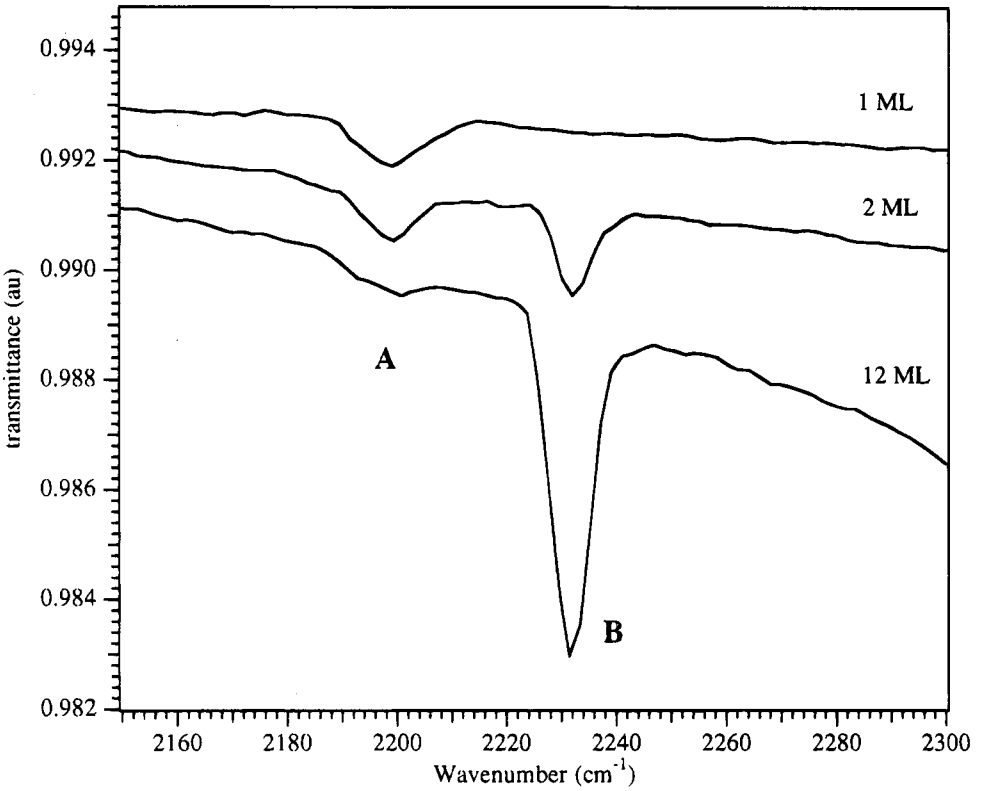

Figure 12. FT-IR spectra of acrylonitrile on Pt(111) for 1 ML, 2 ML, and a multilayer (12 ML) in the C≡N stretching domain. Peak B at 2232 cm^{-1} is assigned to the free C≡N group symmetric stretching.

one expects the hybridization between the lpN°° orbital and the metal to influence the charge density along the C≡N bond.

5. Discussion. We have seen from the NEXAFS results obtained on Au(111) and Pt(111) that the acrylonitrile monolayer is oriented nearly flat on these surfaces. On Au(111), no changes are observed on the antibonding states, showing that the molecules are simply physisorbed on the metal. The UPS results confirm this point: the valence bands of acrylonitrile are preserved during the adsorption.

Concerning the Pt(111) surface, the NEXAFS results have shown that the π^*_{1z} orbital remains similar to the multilayer upon adsorption. On the contrary, the nitrogen lone pair orbital is not observed in UPS at 1 ML, and a new antibonding level with a pronounced *xy*-symmetry appears in the NEXAFS spectra for this coverage, to the right of the π^*_{xy}(C≡N) peak. The fact that this level is not observed at the carbon edge shows that it is very localized on the nitrogen atom. The NEXAFS results show that a strong interaction appears between nitrogen and the metal adsorption site, via the nitrogen lone pair, as indicated by UPS. If this level—which is mainly built on the N(p_x) atomic orbital (taking *x* along the C≡N bond)—hybridizes with a platinum unfilled level, this will give rise to a new antibonding

orbital with an *xy*-symmetry (coming from the p_x character of the lpN°° level). Moreover, considering the initial ordering of the valence levels, the energy position of this antibonding orbital should be located above the π^*_{xy}(C≡N) transition, as observed. The bonding counterpart of this hybridization gives rise to a deeper valence level, so that the lpN°° band is shifted and probably lies underneath other spectral features of the UP spectra. The IR experiments have also shown a weakening of the C≡N bond due to a change of the charge density along the group, that can also be related to the lpN°° hybridization.

Concerning the metal side, the difference between the Au(111) and Pt(111) NEXAFS and UPS results indicates that the top of the d band, an e_g-type orbital which is only partially filled in the case of Pt(111),[16] is involved in this hybridization.

Contrary to the case of ethylene, the HOMO and LUMO of acrylonitrile do not interact with the metal, whereas their energy positions would favor an hybridization with the metal bands around the Fermi level. We can suppose intuitively that the strong delocalization of the frontier orbitals along the molecule prevents or weakens an attractive interaction with the metal, due to a small overlap with the metal bands compared to the case of a localized state. This decreases the charge transfer that could arise from an hybridization between the LUMO and a filled metallic level or between the HOMO and an unfilled metallic level. Moreover, such extended orbitals impose constraining conditions on the adsorption geometry to be in a stabilizing situation over all the metal sites. On the contrary, for small molecules where the MO's are strongly localized on the bond, the molecule can easily interact with one metal site (the π-bonding mode of ethylene at 50 K) or two metal sites (the di-σ bonding mode of ethylene at 95 K) without such symmetry constraints. At last, the localized character of the nitrogen lone pair could explain why this level so strongly interacts with the top of the valence band, whereas its energy position does not favored this interaction.

Conclusion

This work has shown that acrylonitrile is adsorbed flat on the surface and is only physisorbed on Au(111) but is chemisorbed on Pt(111). The chemisorption comes mainly from the interaction of the nitrogen lone pair orbital with the surface. The hybridization between this orbital and the top of the metal valence band leads to a new discrete antibonding level with an *xy*-symmetry observed on the NEXAFS spectra, correlated with the disappearance of the nitrogen lone pair in the UP spectra. A change of the C≡N stretching frequency has also been observed by FT-IR, related to the lpN°° hybridization.

Contrary to the case of ethylene, the HOMO and LUMO of acrylonitrile are not involved in the interaction. The comparison between ethylene and acrylonitrile clearly shows the limitation of the "frontier orbital" model to explain the surface interactions of large molecules containing multifunctional groups.

References and Notes

(1) Cassuto, A.; Mane Mane; Jupille, J.; Tourillon, G.; Parent, Ph. *J. Phys. Chem.* **1992**, *96*, 5987.

(2) Cassuto, A.; Mane Mane; Tourillon, G.; Parent, Ph.; Jupille, J. *Surf. Sci.* **1993**, *287/288*, 460.

(3) Cassuto, A.; Hugenschmidt, M. B.; Parent, Ph.; Laffon, C.; Tourillon, G. *Surf. Sci.* **1994**, *310*, 390.

(4) Delbec, F.; Sautet, P. *Surf. Sci.* **1993**, *295*, 353.

(5) Outka, D. A.; Stöhr, J. *J. Chem. Phys.* **1988**, *88*, 3539.

(6) Detailed ab-initio calculations of the electronic structure and of the NEXAFS transitions have been performed using the Xα-multiple scattering formalism. Laffon, C.; Ehrke, U.; Parent, Ph.; Wurth, W.; Tourillon, G. To be published.

(7) Outka, D. A.; Stöhr, J.; Madix, R. J.; Rotermund, H. H.; Hermsmeier, B.; Solomon, J. *Surf. Sci.* **1987**, *185*, 53.

(8) Miranda, M. P.; Beswick, A.; Parent, Ph.; Laffon, C.; Tourillon, G.; Cassuto, A.; Nicolas, G.; Gadea, F. X. *J. Chem. Phys.* **1994**, *101*, 5500.

(9) Stöhr, J. *NEXAFS Spectroscopy*; Springer Series in Surface Sciences 25; Springer Verlag: Berlin Heidelberg, 1992; Chapter 6.

(10) Jorgensen, W. L.; Salem, L. *The Organic Chemist's Book of Orbitals*; Academic Press: New York and London, 1973.

(11) Neumann, A.; Rabus, H.; Arvanitis, D.; Solomun, T.; Christmann, K.; Baberschke, K. *Chem. Phys. Lett.* **1993**, *201*, 108.

(12) Kimura, K.; Katsumata, S.; Achiba, Y.; Yamazaki, T. *Handbook of He I photoelectron spectra of fundamental organic molecules*; Japan Scientific Society Press: Tokyo, 1981.

(13) Bieri, G.; Åsbrink, L.; von Niessen, W. *J. Electron Spectrosc. Relat. Phenom.* **1980**, *20*, 149.

(14) Delwiche, J.; Gochel-Dupuis, M.; Collin, J. E.; Heinesch, J. *J. Electron Spectrosc. Relat. Phenom.* **1993**, *66*, 65.

(15) Schrader, B.; Meier, W. *Raman/IR Atlas of Inorganic Compounds*; Verlag Chemie: Weinheim, Germany, 1977; Vol. 1.

(16) Banholzer, W. F.; Park, Y. O.; Mak, K. M.; Masel, R. I. *Surf. Sci.* **1983**, *128*, 176.

JP941987S